

A Drug Delivery System for Administration of Anti-TNF- α Antibody

Marie-Claude Robert^{1,2}, Mathieu Frenette³, Chengxin Zhou¹, Yueran Yan⁴, James Chodosh¹, Frederick A. Jakobiec^{1,5}, Anna M. Stagner^{1,5}, Demetrios Vavvas⁴, Claes H. Dohlman^{1,2}, and Eleftherios I. Paschalis^{1,2}

¹ Massachusetts Eye and Ear Infirmary, Department of Ophthalmology, Harvard Medical School, Boston, MA, USA

² Massachusetts Eye and Ear Infirmary/Schepens Eye Research Institute, Boston Keratoprosthesis Laboratory, Harvard Medical School, Boston, MA, USA

³ Université du Québec à Montréal, Department of Chemistry, Montreal, QC, Canada

⁴ Massachusetts Eye and Ear Infirmary, Department of Ophthalmology, Angiogenesis Laboratory, Harvard Medical School, Boston, MA, USA

⁵ Massachusetts Eye and Ear Infirmary, David G. Cogan Laboratory of Ophthalmic Pathology, Harvard Medical School, Boston, MA, USA

Correspondence: Eleftherios Paschalis, Department of Ophthalmology, Boston Keratoprosthesis Laboratory, Massachusetts Eye and Ear Infirmary and Schepens Eye Research Institute, Harvard Medical School, Boston, MA 02114, USA. e-mail: eleftherios_paschalis@meei.harvard.edu

Received: 19 June 2015

Accepted: 09 February 2016

Published: 11 March 2016

Keywords: polydimethylsiloxane; tumor necrosis factor alpha; drug delivery system; biologics; sustained-release; burn

Citation: Robert MC, Frenette M, Zhou C, et al. A drug delivery system for administration of anti-TNF- α antibody. 2016;5(2):11, doi:10.1167/tvst.5.2.11

Purpose: To describe the fabrication, evaluation, and preliminary in vivo safety of a new drug delivery system (DDS) for topical anti-TNF- α antibody administration.

Methods: A DDS was fabricated using inverse template fabrication of a hydrophobic three-dimensional porous scaffold (100–300 μm in diameter porosity) loaded with 10% polyvinyl alcohol hydrogel carrying 5 mg/ml (weight/volume) of anti-TNF- α antibody. Drug-loaded DDS was sterilized with 25 kGy of gamma irradiation. Long-term in vitro antibody affinity and release was evaluated at room temperature or 37°C using enzyme-linked immunosorbent assay (ELISA) and protein fluorescence. In vivo clinical and histopathological assessment was performed by subcutaneous implantation in BALB/c mice for 3 months.

Results: Gamma irradiation, repeated dry/wet cycles, and storage at room temperature for 1 year or 37°C for 1 month had no deleterious effects on antibody affinity. Anti-TNF- α release was high during the first minutes of aqueous exposure, followed by stabilization and gradual, low-dose, antibody release over the next 30 days. Histopathologic evaluation of explanted DDS showed a fibrous pseudocapsule and a myxoid acute/chronic inflammation without granuloma formation surrounding the implants.

Conclusions: Sustained local delivery of anti-TNF- α antibody is feasible using the described DDS, which provides stability of the enclosed antibody for up to 1 year of storage. Preliminary results show good in vivo tolerance following subcutaneous placement for 3 months. The proposed fabrication and sterilization process opens new possibilities for the delivery of biologic agents to the anterior surface of the eye.

Translational Relevance: The described DDS will facilitate the treatment of ocular surface diseases amenable to biologic therapy.

Introduction

Biologic agents targeting key cytokines and growth factors are being applied to an expanding spectrum of human systemic diseases and ocular disorders. For example, intravitreal injection of anti-vascular endothelial growth factor (VEGF) agents has become the gold standard of treatment of choroidal neovascularization and diabetic macular edema.^{1–4} Applications

of anti-VEGF therapy are also currently being investigated for several ocular surface conditions including corneal neovascularization,⁵ pterygium,⁶ and high-risk penetrating keratoplasty.⁷

Likewise, monoclonal antibody against tumor necrosis factor alpha (TNF- α), such as infliximab (Janssen Biotech, Inc., Horsham, PA), is an interesting therapeutic approach to the targeted treatment of ocular surface diseases. Indeed, TNF- α is a pleotropic

cytokine with important contributions in the pathogenesis of inflammation, angiogenesis, and collagenolysis.^{8–10} Systemic administration of infliximab has been reported to stabilize corneal melting in patients with autoimmune diseases (rheumatoid arthritis, Crohn disease, peripheral ulcerative keratitis) that were recalcitrant to other treatment modalities.^{11–14} Intravenous infliximab has also improved the retention of the Boston Keratoprosthesis, an artificial cornea, in patients with Stevens-Johnson syndrome or rheumatoid arthritis and recurrent corneal melt.^{15–17} Further, a single intraperitoneal dose of 6.25 mg/kg of anti-TNF- α in mice inflicted with alkali corneal burns significantly reduced corneal inflammation, neovascularization, and inhibited retinal ganglion cell layer apoptosis as compared with isotype IgG treatment control.¹⁸

A limitation to the use of biologic therapies is the risk of significant systemic adverse events. Local administration achieves lower systemic exposure to the drug and therefore is likely associated with lower rates of severe adverse events. The use of infliximab eye drops has been investigated as an alternative modality for local drug delivery. The administration of topical infliximab eye drops reduced corneal opacity, perforation, and eyelid fibrosis in a mouse model of corneal alkali burn,¹⁹ and improved tear volume, corneal surface regularity, and goblet cell density in a mouse model of dry eye.²⁰ In rabbit models, the use of topical infliximab prevented corneal neovascularization²¹ and suppressed subconjunctival wound healing after trabeculectomy.²² On the other hand, cerebrovascular accidents are recognized complications of systemic anti-VEGF therapy²³ while anti-TNF- α agents are associated with a risk of opportunistic infections, malignancies, infusion reactions, as well as cardiac and renal toxicity.^{24,25} Local administration achieves lower systemic exposure to the drug, and therefore is likely associated with lower rates of severe adverse events. For example, the risk of arterial thromboembolic events is approximately 3% with intravitreal bevacizumab administration but increases to 10% with intravenous use.^{26,27} The sustained and selective release of biologics to diseased tissue using drug-eluting carriers is a promising therapeutic alternative for maximizing bioavailability while minimizing side effects. However, the direct delivery of biologic agents to the front of the eye is challenging. The large molecular size (~ 150 kD) and the hydrophilic nature of antibodies limit corneal epithelial penetration, and thus, limit the bioavailability to the corneal stroma and the rest of the

anterior segment. The use of a drug-eluting polymer placed on the ocular surface prolongs the precorneal residence time of the medication, and is thus one approach to improve antibody penetration when compared with eye drops.²⁸ This effect is even more important for ocular diseases that cause epithelial barrier loss. Further, product sterilization is an outstanding challenge in the manufacture and in vivo application of biologic drug-eluting polymers. Heat or gas sterilization processes may damage protein structure and alter the antibody's antigen binding affinity or modify the systemic response to the biologic agent, thereby limiting the manufacturing options and increasing the cost of biologic drug-eluting polymers.^{29,30}

The purpose of this study was to develop an anti-TNF- α drug delivery system (DDS) and to test gamma irradiation as an alternative method of post manufacturing sterilization. Moreover, drug stability and release were examined in vitro while in vivo adverse effects were evaluated histopathologically following subcutaneous implantation in mice.

Materials and Methods

Preparation of the DDS

A three-dimensional (3D) porous polydimethylsiloxane (PDMS) block was prepared as previously described.³¹ Water dissolvable particles with a diameter between 100 and 300 μm were used to create the negative PDMS template. The particles were dissolved by agitation in 95°C water for 3 hours resulting to an interconnected porous PDMS network (Fig. 1), as determined by nondestructive 3D x-ray micro-computed-tomography (X-Tek HMXST225; Nikon Metrology Inc., Brighton, MI), and 3D image reconstruction (VGStudio Max 2.2; Volume Graphics, Heidelberg, Germany; Fig. 1). The sponge-like microporous PDMS provided 50% cavitation volume and was sectioned into small segments of 5 mg ($\sim 5 \times 2 \times 1$ mm).

Polyvinyl alcohol (PVA) 10% wt/vol loading polymer was prepared as follows: PVA powder (# 363,146-500G; Sigma Aldrich, St. Louis, MO) was slowly added into deionized (DI) water and stirred on a hotplate, heating up to 90°C to 98°C until the PVA powder was totally dissolved. The mixture was cooled to room temperature (RT) and infliximab lyophilized powder (a chimeric monoclonal anti-TNF- α antibody) was suspended at a 34:1 wt/vol ratio (infliximab:PVA solution) resulting in an anti-TNF-

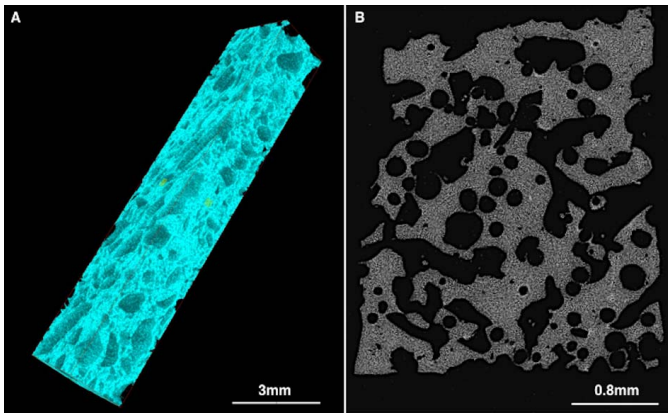


Figure 1. X-ray microtomography of the porous PDMS. (A) Macroscopic and (B) microscopic appearance of porous PDMS. The microstructure of PDMS was determined using nondestructive, molybdenum-generated radial x-ray scans. Three-dimensional image reconstruction of the microcomputed-tomography (μ CT) was achieved using VGStudio Max 2.2 image reconstruction software. The porous cavities are subsequently loaded with infliximab using polyvinyl alcohol as a loading polymer.

α antibody concentration of 5 mg/ml. The polymer was then loaded into the 3D microporous PDMS using a vacuum chamber and air-dried (Fig. 2).

The infliximab-loaded PDMS DDS was stored at room temperature until use. Gamma irradiation was

applied to select DDSs used in the drug release assays and to all DDSs used in the in vivo assays given the need for sterilization of the device. A Cobalt-60 source was used to deliver a total dose of 25 kGy, which is the standard requirement for tissue sterilization.

Anti-TNF- α Stability and Release From the Drug Delivery Device

The stability and release of infliximab were evaluated using a commercially available sandwich enzyme-linked immunoassay (ELISA; Quantikine Human TNF- α Immunoassay; R&D Systems, Minneapolis, MN). The assay protocol was modified to include a 1-hour incubation at 37°C to allow antigen-antibody binding between a known quantity of TNF- α (125 pg/mL) and the infliximab eluted from the DDS TNF- α bound by infliximab through antibody-antigen interaction is unable to bind to the capture antibody coating of the ELISA well and is, therefore, washed away during the subsequent steps of the assay. The remaining TNF- α in the solution, which was not bound by anti-TNF- α antibody, is then measured using the standard steps of the assay.^{32,33} The amount of TNF- α bound by infliximab is then calculated by subtraction from the initial amount of

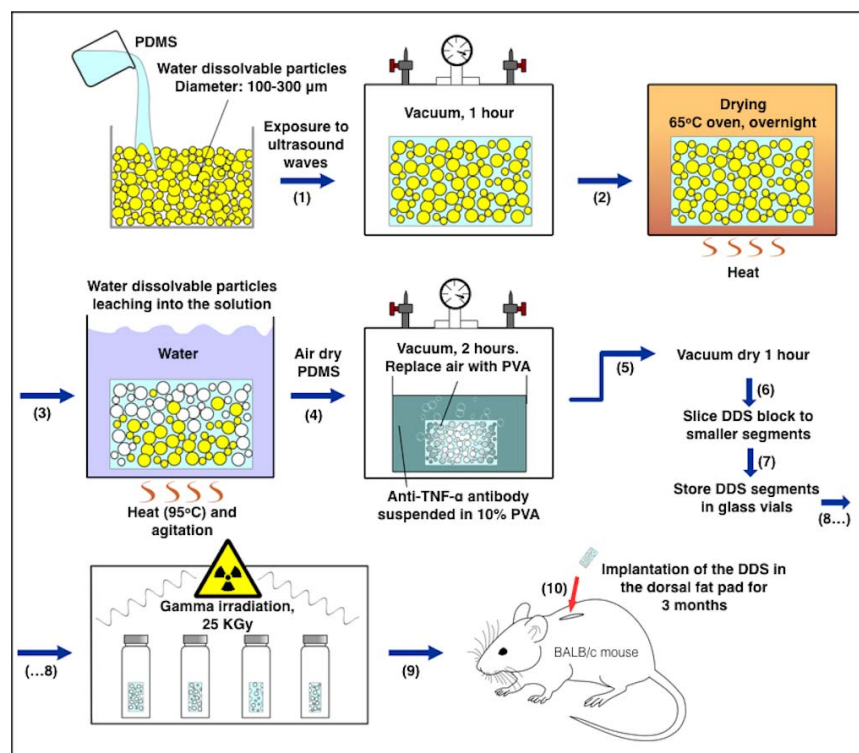


Figure 2. Manufacturing sequence of the anti-TNF- α drug delivery system (DDS).

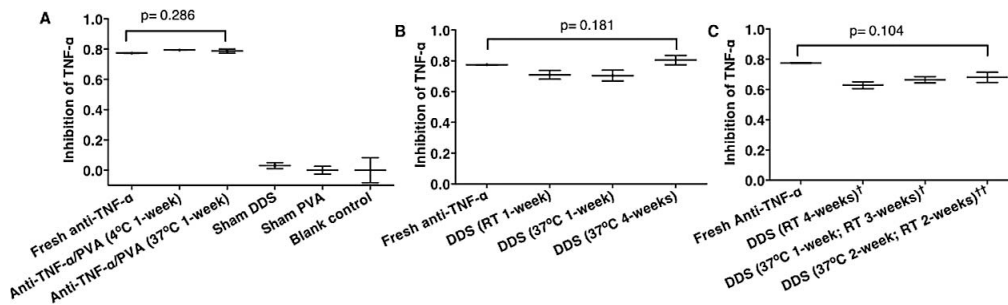


Figure 3. Stability of anti-TNF- α antibody in the drug delivery system. (A) Infliximab in polyvinyl alcohol (4 μ g/mL) following 1 week at 4°C or 37°C has similar TNF- α binding affinity and inhibition when compared with freshly prepared 4 μ g/mL infliximab. TNF- α inhibition with and without blank PVA or PDMS is negligible, demonstrating that neither polymer adsorbs TNF- α nor interfere with the assay. (B) Infliximab in PDMS is stable after 1 week at RT as well as 1 and 4 weeks at 37°C. (C) Stability of anti-TNF- α loaded PDMS after 4 weeks at RT or 37°C following repeated cycles of incubations in 125 pg/mL TNF- α solution and air-drying ([†]one cycle, ^{††}two cycles).

TNF- α loaded into each well. Anti-TNF- α antibody activity was quantified as the percentage of captured TNF- α (percent TNF- α inhibition): [125 pg/mL minus TNF- α concentration measured by ELISA] divided by 125 pg/mL). A standard curve was prepared with each assay using TNF- α concentrations between 0 and 125 pg/mL. The percentage of TNF- α inhibition was compared with inhibition values for known infliximab concentrations varying between 0 and 5000 ng/mL. The relationship between infliximab concentration and TNF- α binding to the ELISA was modeled with the following standard curve (allometric equation): infliximab concentration (y) = 0.05426 \times (optical density)^{-4.51279}, $R^2 = 0.99$. The infliximab standard curve remained within the validated detection range of TNF- α (15.6 – 1000 pg/mL) for the ELISA. All measurements were performed in triplicate.

The stability of the anti-TNF- α antibody was assessed under different conditions. First, the anti-TNF- α /PVA loading polymer mixture was evaluated after dry storage for 1 week at 4°C and 37°C. On the day of the assay, the anti-TNF- α /PVA loading polymer was diluted in normal saline to an infliximab concentration of 4 μ g/mL, mixed 50:50 with 250 pg/mL TNF- α (effective concentration of 125 pg/mL of TNF- α) and incubated for 1 hour at 37°C. The percentage of TNF- α inhibition using ELISA was calculated as described above. Also, the DDS was evaluated after dry storage at room temperature (RT) or 37°C for up to 4 weeks. The DDS was submerged and incubated in 400 μ L of 125 pg/mL TNF- α for 1 hour at 37°C and the soaking solution was used for the subsequent ELISA. Fresh infliximab solution (4 μ g/mL, lyophilized powder dissolved in normal saline) was prepared as a positive control.

Sham PVA and sham DDS (without infliximab) were used as controls to ensure that the polymers did not adsorb or neutralize significant amounts of TNF- α . Sham PVA (PVA 10% without infliximab) was prepared and stored at 4°C for 1 week (Fig. 3A). Sham PVA was diluted in normal saline using the same dilution factor used for anti-TNF- α /PVA. The diluted sham PVA was mixed with TNF- α , incubated for 1 hour at 37°C and used for the subsequent ELISA. Sham DDS were prepared, sectioned into 5-mg segments and stored at RT for 4 weeks prior to being assayed. Using an identical technique to infliximab loaded DDS, sham DSS segments were submerged and incubated in 400 μ L of 125 pg/mL TNF- α solution for 1 hour at 37°C. The soaking solution was used for the subsequent ELISA.

Three segments of the DDS were used to assess drug release and stability after serial assays and wet-dry cycles over a 4-week period. After 1 or 2 weeks of dry storage at RT or 37°C, the segments were incubated with 125 pg/mL TNF- α at 37°C for an hour. The soaking solution was used for the ELISA assay while the DDS segments were recovered, air-dried, and stored at RT until a repeat assay was performed.

To assess the drug-eluting properties of the DDS, 5-mg segments of the polymer were sequentially soaked in either 500 μ L or 1000 μ L of 0.9 % normal saline and incubated at 37°C for a 10-day period. The volume of soaking solution did not significantly alter the release of infliximab (Supplemental Fig. S1). Wherein infliximab is known to completely dissolve at a concentration of 10 mg/mL,¹⁰ the expected amount of infliximab present in the DDS would only achieve concentrations in the μ g/mL scale. Thus, the 500 and 1000 μ L volume achieves sink conditions.

Nongamma- and gamma-irradiated DDS segments were each sequentially transferred to fresh soaking solution (500 μ L) at predetermined time-points over a 1-month period. These included 3 and 24 hours as well as 2, 4, 6, 8, 10, 12, 15, 17, 20, 22, 25, 28, and 31 days after preparation. The different soaking solutions were stored at 4°C until the day of the assay. Each soaking solution, which contained infliximab released from the DDS, was allowed to react with equal volume of 250 pg/mL TNF- α (final TNF- α concentration of 125 mg/mL) for 1 hour at 37°C prior to proceeding with the ELISA using the standard protocol. This drug-elution experiment was repeated using nongamma- and gamma-irradiated DDS that had previously been stored at RT for 1 year.

Given the limitations in quantifying the early release of high concentrations of infliximab using ELISA, quantification of infliximab protein eluted from the DDS was also performed using fluorescence spectroscopy with measurement of the infliximab fluorescence signal at 340 nm, using an excitation wavelength of 280 nm. First, the real-time elution characteristics were evaluated using constant monitoring of fluorescence measurements over 2 hours of a freshly prepared DDS placed inside a 1 \times 1 cm quartz cuvette containing 1.5 mL of 0.9% normal saline with constant agitation using a magnetic stirrer. The long-term release of infliximab was assessed by soaking the DDS in 1000 μ L of normal saline at RT without stirring. Sequentially, the DDS was transferred to fresh normal saline over a 35-day period (at days 1, 3, 7, 14, 23, and 35). Fluorescence spectroscopy was performed on each of the soaking solutions and the amount of released infliximab was calculated as micrograms of anti-TNF- α antibody per day of soaking.

In Vivo Tolerance of the Drug Delivery Device

In vivo studies were approved by the Animal Care Committee of the Massachusetts Eye and Ear Infirmary. All animal-based procedures were performed in accordance with the ARVO Statement for the use of Animals in Ophthalmic and Vision Research, and the National Institutes of Health Guidance for the Care and Use of Laboratory Animals.

All procedures were performed under general anesthesia using intraperitoneal ketamine (120 mg/kg; Putney Inc., Portland, ME) and xylazine (20 mg/kg; Vedco Inc., St. Joseph, MO) as previously

described.¹⁸ Postoperative analgesia was provided using subcutaneous buprenorphine hydrochloride (0.05 mg/kg, Buprenex Injectable; Reckitt Benckiser Healthcare, Ltd., Slough, UK).

In order to preliminarily assess the in vivo safety, sections of the gamma-irradiated DDS were surgically implanted in the subcutaneous space of the dorsal fat pad in two BALB/c male mice and kept in situ for 3 months. Sham DDS without anti-TNF- α antibody was implanted in two separate BALB/c male mice as polymer controls. At 3 months, the DDS were explanted for further clinical and histopathologic analysis. The DDS and surrounding tissue was sectioned and stained with hematoxylin-eosin and Masson trichrome.

Statistical Analysis

Statistical analysis was performed using GraphPad Prism software (San Diego, CA). The inhibition of TNF- α by released infliximab was compared between time point and storage conditions using the nonparametric Kruskal-Wallis (KW) test. Dunn's multiple comparisons test was performed for each pair of the testing conditions if the *P* value was below 0.05. Per convention, a two-tailed *P* value below 0.05 was defined as being statistically significant. Bonferroni correction was applied as appropriate.

Results

Stability Evaluation of Drug Delivery Device

Quantification of infliximab, performed using a validated ELISA assay,³² revealed stable binding to TNF- α following storage in various conditions. Infliximab-PVA (4 μ g/mL) stored for 1 week at either 4°C or 37°C had similar TNF- α inhibition when compared to freshly prepared infliximab (4 μ g/mL) with TNF- α inhibition of 79.4% \pm 0.2%, 78.7% \pm 1.3%, and 77.4% \pm 0.1%, respectively (*P* = 0.286; KW test). PVA without infliximab did not show any inhibition of TNF- α (0.0% \pm 2.9%; Fig. 3A).

The 5-mg DDS segments stored at RT or 37°C for 1 week inhibited 71% \pm 3% and 70% \pm 3% of the TNF- α , respectively. The level of TNF- α inhibition after 4 weeks at 37°C was not significantly changed (80.5% \pm 3%, *P* = 0.181; KW test). Further, sham DDS (without anti-TNF- α) did not lead to significant inhibition of TNF- α (3.0% \pm 1.9%; Fig. 3B). DDS, stored at RT and/or 37°C for 4 weeks, continued to show 63% to 68% inhibition of TNF- α despite

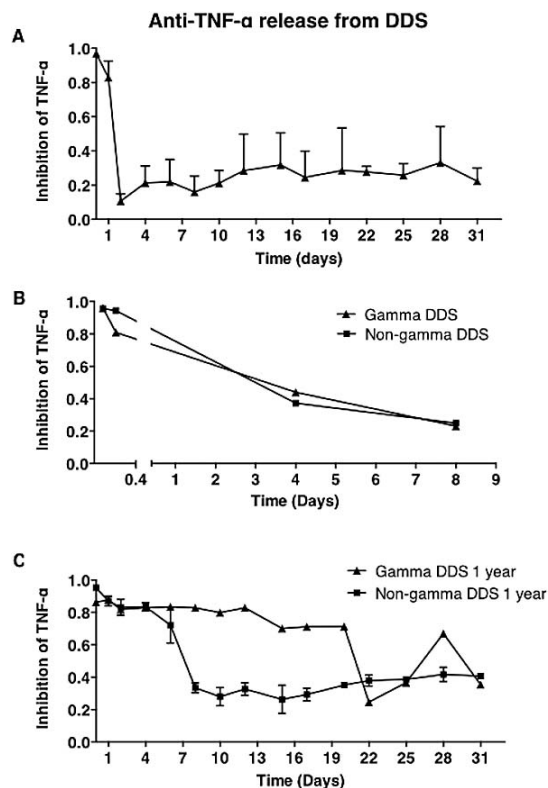


Figure 4. Anti-TNF- α antibody release after continuous aqueous exposure of the drug delivery system. (A) The release of biologically active anti-TNF- α antibody from the drug delivery system (DDS) over 31 days is quantified as the relative inhibition of TNF- α (125 pg/mL). Due to burst release of anti-TNF- α antibody, TNF- α inhibition was almost complete after the initial 3-hour soaking period. High levels of anti-TNF- α antibody were released in the next 24 hours, followed by lower but stable zero-order release for the subsequent 30 days. (B) Gamma irradiation with 25 kGy did not impede the release characteristics or the anti-TNF- α antibody or the binding affinity when compared with nongamma-irradiated DDS. (C) After 1 year of shelf storage, nongamma- as well as gamma-irradiated DDS showed preserved inhibition of TNF- α . The release curve shows prolongation of the initial burst release of anti-TNF- α antibody, which is particularly marked for the gamma-irradiated DDS.

previous repeated dry-wet cycles and incubation with TNF- α solution ($P = 0.104$; KW test; Fig. 3C).

Anti-TNF- α Release from Drug Delivery Device

As shown in Figure 4, the release of biologically active anti-TNF- α antibody from the DDS in the first 3 hours of soaking was significant. TNF- α inhibition was almost complete ($96.9\% \pm 0.8\%$) and exceeded the lower detection limit of the assay. At 24 hours, release of infliximab remained high with $82.8\% \pm 9.8\%$ inhibition of TNF- α , corresponding to an

infliximab release of $2.11 \mu\text{g}/\text{day}$. Lower levels of drug release occurred at zero order kinetics for the following 30 days. During this period (days 2–31), average TNF- α inhibition was $24\% \pm 6\%$ and corresponded to infliximab release of $1.23 \pm 0.29 \text{ ng}/\text{day}$ (Fig. 4). Gamma-irradiated DDS had similar infliximab release and TNF- α inhibition characteristics when compared with nongamma-irradiated DDS (Fig. 4B). Further, nongamma- and gamma-irradiated DDS that had been kept at RT for 1 year showed a retained ability to release biologically active infliximab (Fig. 4C). The release curve showed high levels ($>80\%$) of TNF- α inhibition for the first 4 and 12 days of continuous aqueous exposure for the nongamma- and gamma-irradiated DDS, respectively. In contrast, freshly prepared DDS only exhibited this level of TNF- α inhibition over the first 24 hours.

Using an excitation wavelength of 280 nm, the fluorescence signal of freshly prepared infliximab in normal saline at 340 nm was linearly correlated to infliximab concentrations between 0 to $36.3 \mu\text{g}/\text{mL}$ ($R^2 = 0.999$; Fig. 5A). Real-time monitoring of infliximab release from DDS of 5 mg total weight revealed that the burst release occurred within the first 30 minutes of soaking and that slow elution continued thereafter (Fig. 5B). A total of $44.9 \mu\text{g}$ of infliximab was released over the 2-hour assay. The 35-day infliximab release curve reveals significant early antibody release ($27.2 \mu\text{g}/\text{day}$ over first 24 hours), stabilization of the release kinetics between days 7 and 14, followed thereafter by zero-order release ($23 \pm 6 \text{ ng}/\text{day}$ between days 14 and 35; Fig. 5C).

In Vivo Tolerance of the Drug Delivery Device

A DDS ($5 \times 2 \times 1 \text{ mm}$ in size) was implanted subcutaneously beneath the dorsal fat pad in two anesthetized BALB/c mice without complication. The mice were observed for 3 months and did not show evidence of clinical inflammation, infection, skin necrosis, or systemic illness. After 3 months, the explanted DDS with and without anti-TNF- α antibody showed similar histopathological findings (Fig. 6). The implants were found to have been inserted either in a premuscular plane or underneath multiple layers of striated muscle cells. A thin and irregular translucent lamina of DDS residue was adherent to the tissue edges, but most of the device had been dislodged or dissolved during tissue processing. Fibroblastic proliferation was detected in the host tissues immediately surrounding the implants and

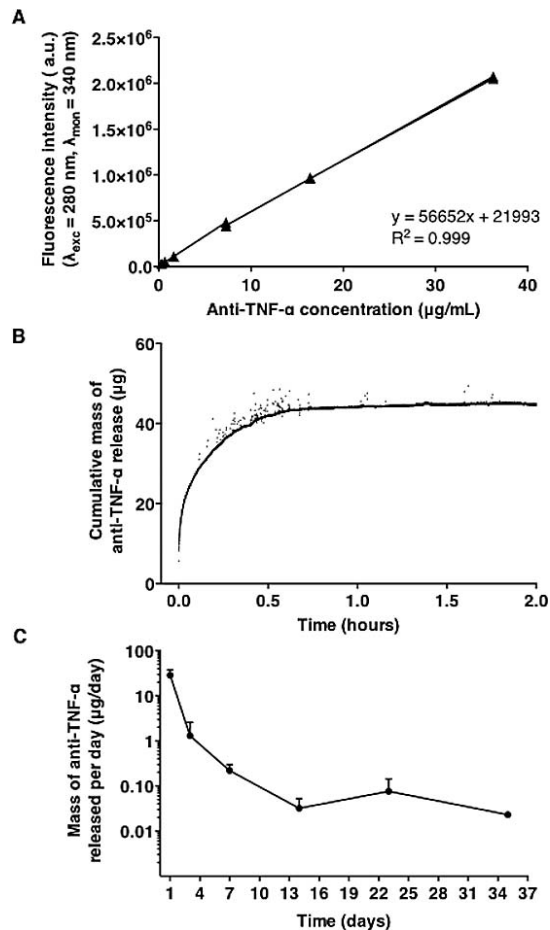


Figure 5. Release of anti-TNF- α antibody from the drug delivery system using fluorescence spectroscopy. Fluorescence calibration curve for anti-TNF- α antibody in normal saline buffer (excitation wavelength of 280 nm, monitoring wavelength [λ] of 340 nm). The fluorescence signal linearly correlates to concentrations of freshly prepared anti-TNF- α antibody between 0 and 80 $\mu\text{g/mL}$ ($R^2 > 0.99$). (B) Real-time quantification of released anti-TNF- α antibody from a 5 mg total weight DDS placed into 1.5 mL of normal saline at room temperature as measured by fluorescence. (C) Fluorescence quantification of anti-TNF- α antibody released from 5 mg total weight DDS placed into 0.5 mL of normal saline at room temperature over 35 days.

manifested little evidence of collagen synthesis as revealed by the Masson trichrome stain which demonstrated the absence of blue stain interstitial fibrillar material (Fig. 6A). The fibroblastic pseudocapsule was most compact at the superficial edge and looser at the base and lateral edges of the implant. The spindle cells responsible for the pseudocapsule appeared to be myofibroblasts in view of their cytoplasmic fuchsinophilia with the Masson trichrome stain. A mixed mononuclear and polymorphonuclear leukocytic inflammatory response was

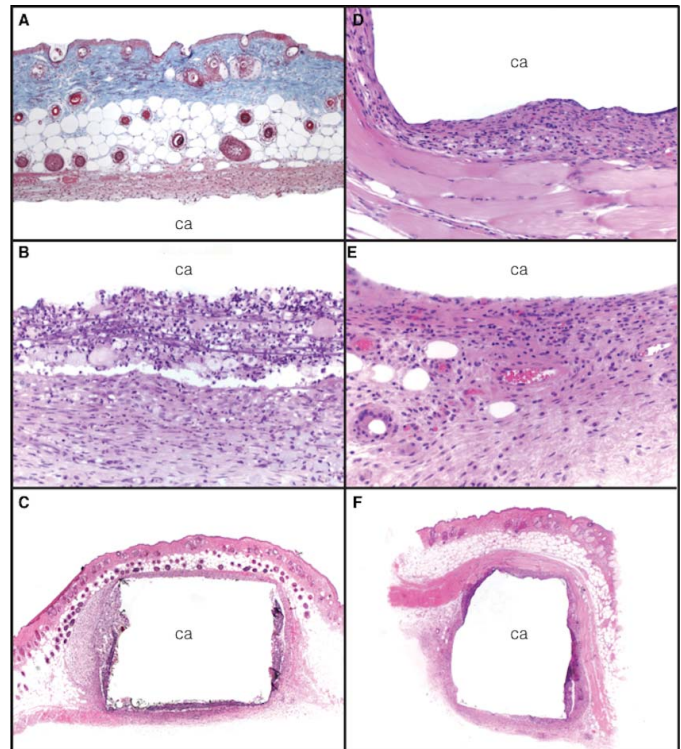


Figure 6. Histopathologic findings of implanted with anti-TNF- α antibody (A–C) DDS and sham DDS (D–F). (A) Masson trichrome stain discloses that the collagen of the dermis is *blue*. The subdermal fat bearing cross sections of hairs is uninfamed. Note the pseudocapsule lining the implant cavity (ca) below is lightly red staining and lacks blue staining collagen as well as prominent capillaries. (B) Upon the inside surface of the pseudocapsule below rests an exudative inflammatory process with suspended acute and chronic inflammatory cells. Similar cells are also present in the more compact fibroblastic pseudocapsule devoid of capillaries. DDS cavity (ca). (C) Cavity of an explanted DDS (ca) that contained anti-TNF- α antibody. The implant encroaches on the subcutaneous fat with hairs and was located above the striated muscle. An inflammatory exudate with suspended cells is apparent multifocally, especially on the inside of the fibroblastic pseudocapsule at the lateral and vertically oriented edges. There is considerable myxoid change in the fat on the left adjacent to the cavity. Striated muscle is revealed as an uninfamed eosinophilic band below the cavity. (D) More compact zone of cavity wall beneath striated muscle fibers below. (E) Bland stromal cells and scattered mononuclear inflammatory cells constitute the wall delimiting the cystic cavity below. Several small capillaries can be seen in the wall. DDS cavity (ca). (F) Low power photomicrograph of cavity (ca) that had a DDS without anti-TNF- α antibody. The epidermis and dermis are present on the *top*, beneath which is a layer of uninfamed fat. The implant is located beneath the subcutaneous musculature. ([A–D, F] hematoxylin and eosin, $\times 50$, $\times 200$, $\times 200$, $\times 50$, $\times 200$; [E] Masson trichrome, $\times 100$).

observed in multiple foci along the inner aspect of the fibrous pseudocapsule (Fig. 6B). The implants with anti-TNF- α antibody (Fig. 6A–C) showed somewhat greater inflammation immediately abutting the DDS. The implants without anti-TNF- α antibody (Fig. 6D–F) had a slightly greater presence of capillaries in the vicinity of the implant. In one of these infliximab-loaded implants, a focus of myxoid reaction containing acute and chronic inflammation was seen in the adjacent fat. Granulomatous zones were not observed around or near the implants.

Discussion

We describe the preparation of a novel DDS made of PDMS/PVA for topical delivery of anti-TNF- α antibodies and demonstrate its biological stability, drug-release characteristics, and in vivo tolerability. Further, we establish that post production exposure of the DDS to gamma irradiation may be a feasible sterilization option without undue consequences to the antibody's affinity and biological activity.

Local administration of anti-TNF- α requires lower doses than systemic administration, thus minimizing costs and the risk of systemic complications. For the cornea, the short drug residence time achieved with eye drops due to normal tear flow and reflex tearing are important barriers to achieving sufficient drug concentrations in the target tissue. This is especially true with larger hydrophilic molecules such as biologic agents. Subconjunctival administration is able to achieve greater bioavailability but involves an invasive procedure.³⁴ Other systems have been developed for sustained drug delivery to the ocular surface. For example, colloidal formulations such as liposomes and nanoparticles can be designed to improve corneal penetration and drug stability.³⁵ While improving bioavailability, these thicker formulations may cause visual blurring by adhering on the corneal surface upon instillation, which in turn, may harm patient compliance. Contact lenses have also been used for the release of several therapeutic agents including antibiotics and glaucoma drugs.^{36,37} However, the needs of optical clarity, oxygen permeability, and the specific design for fit over the cornea, limit the types of materials and the degree of customization that is otherwise possible with other drug delivery systems.³⁸ Dissolvable inserts share a similar approach to the current DDS by prolonging drug residence time on the ocular surface. Drug release and dissolution of these inserts are dependent on hydration and tear flow, which may be highly variable

in patients with inflammatory conditions that would necessitate anti-TNF- α therapy.³⁹ Ocusert, a non-dissolvable lower-lid insert, can be used to deliver pilcarpine medication to the eye. A membrane barrier is used to control the release, which may not be suitable for larger biologic agents.⁴⁰

The delivery of therapeutic proteins, such as anti-TNF- α antibody poses additional challenges including those of drug instability, immunogenicity, and shorter half-lives in the body.³⁰ Various techniques have been employed to stabilize protein, mainly by encapsulating the protein in biodegradable polymers.³⁰ Hydrogels and porous polymeric scaffolds are the two main delivery systems used to provide controlled and sustained protein delivery for longer periods of time. PVA hydrogel is a nontoxic and noncarcinogenic biocompatible hydrophilic polymer suitable for mixing at low temperatures, thus preventing protein denaturation. Further, PVA allows water diffusion at a relatively slow rate causing expansion of the hydrogel and change in release characteristics.⁴¹ However, the PVA structure is less resilient to deformation at increased mechanical stresses, such as occurs during blinking.⁴² On the other hand, polymeric scaffolds can be tailored to deliver drugs for longer durations. However, their manufacturing often involves chemicals and techniques that can cause protein denaturation. PDMS is a popular biocompatible siloxane polymer used for drug delivery. Prepolymer (liquid form) PDMS is often mixed with the drug prior to the curing process. The two important limitations of this system are the use of peroxide or heat to cure the prepolymer and the inability of polar drugs (hydrophilic proteins) to mix well in nonpolar (hydrophobic) PDMS. Therefore, PDMS is preferentially used as drug delivery system of nonbiologic, nonpolar drugs.⁴³ However, cured PDMS holds several advantages. It is mechanically very stable, nondegradable, and biocompatible. PDMS can be used to fabricate polymer scaffolds, suitable for use in tissues that exhibit high mechanical stresses, such as the lid and ocular surface. Its low surface energy (hydrophobicity) prevents wetting by polar liquids. The addition of surface roughness by the porous structure enhances its hydrophobicity.³¹ Hydrophobicity slows penetration of water into the PDMS porous network, thereby preventing rapid hydration and release of the loaded drug.

In the current study, a combination of nonbiodegradable porous PDMS scaffold, loaded with PVA hydrogel that contained anti-TNF- α antibody was used. The preparation of porous PDMS was per-

formed using biocompatible sacrificial particles, as previously described.³¹ The loading technique of anti-TNF- α antibody into PVA was benign and aimed at reducing the risk of protein denaturation. Similarly, PVA loading into the PDMS porous network was performed at low temperatures with negative pressure. Loaded protein was not exposed to cross-linkers, chemicals, or heat during the process. Functional experiments of anti-TNF- α mixed with PVA showed antibody functional stability. In our system, PVA swelling was restricted by the porous PDMS scaffold and water diffusion was further reduced by the low surface energy of PDMS.

Our experiments demonstrate that infliximab can be successfully loaded into a carrier polymer and remains biologically stable when kept at 37°C for up to 1 month. In addition, exposure of the infliximab-PVA-PDMS design to high dose (25 KGy) gamma irradiation was not deleterious to the protein binding affinity, paving the possibility for convenient post manufacturing sterilization. This is particularly important given the historical burden of biologic drug production, requiring pathogen-free production of antibodies to avoid later antibody denaturation during the sterilization process.⁴⁴ Our results using DDS after 1 year of RT shelf storage indicate that the release of biologically active antibody is possible. However, further process optimization of DDS fabrication, storage, and handling is necessary to reduce the variability of infliximab release. This is particularly true for gamma-irradiated DDS.

The release curves obtained through fluorescence spectroscopy and ELISA correlate well with each other, as both quantification methods show a rapid burst of anti-TNF- α antibody released from the DDS which is then followed by slow yet stable release after 1 to 2 weeks. However, as fluorescence measurements are based on native tryptophan fluorescence and not biologically active antibody, this technique overestimates the amount of infliximab released from the DDS when compared with ELISA measurements. The burst of infliximab release is thought to be related to the infliximab/PVA found on the surface of the polymer and can be expected to be higher in an agitated solution. The subsequent slower release rates likely relate to the diffusion of infliximab from inside the PDMS polymer. While the amount of released infliximab appears low, it is important to note that TNF- α is a potent cytokine. It has been shown that a minute quantity of 10 ng/mL of recombinant TNF- α can induce apoptosis.⁴⁵ Conversely, a small amount of locally delivered TNF- α inhibitor can potentially

have biologically relevant and meaningful protective effect on the ocular surface. Preliminary in vivo data have shown detectable levels of infliximab in the DDS after 3 months of subconjunctival implantation in rabbit eyes. Detection of infliximab was performed using monoclonal anti-IgG antibody in tissue sections of the explanted DDS. Explanted sham DDSs showed lack of anti-IgG staining (Zhou C, et al. *IOVS*. 2016; ARVO E-Abstract 1271).

Finally, the DDS failed to show any sign of local or systemic toxicity when implanted subcutaneously for up to 3 months in mice. A mixed-acute and chronic inflammatory cell reaction was noted within the compact fibroblastic pseudocapsule as well as in areas with a more myxoid matrix, particularly in the implant with the chimeric antibody. This may represent a reaction to the chimeric antibody's antigenicity. However, the formation of a fibrous capsule around biomaterial implants is a common phenomenon, and thus, it is not solely due to the antigenicity of anti-TNF- α .⁴⁶ Alternatively, the inflammation may be a consequence of the differential trauma of surgical implantation of the DDS. There were slightly fewer capillaries in the DDS specimen containing anti-TNF- α antibody. This is not surprising as infliximab has been shown to reduce angiogenesis in the corneal stroma.^{4,16} No granulomatous elements were detected near the implants. The implants therefore appeared to be satisfactorily tolerated in vivo. With the passage of time the inflammatory response would have been expected to subside, leaving behind only a quiescent contracted pseudocapsular scar with the progressive deposition of collagen.

The long-term objective is to place the DDS in the conjunctival fornix to circumvent the short precorneal residence time seen with eye drops. It is likely to be well-tolerated while allowing a more targeted and specific approach to ocular surface drug delivery. This would allow the elution of high doses of antibody initially followed by zero-order release for the subsequent month. Further, the use of a carrier polymer might be more attractive to clinicians and patients given its expected ease of insertion and removal into the conjunctival fornix, allowing for titration of therapy as medically necessary and ensuring patient adherence. Alternatively, the DDS could be placed in the subconjunctival space. While this would likely provide better diffusion dynamics and saturation in the eye, this approach is more invasive as it would require the surgical implantation and removal of the polymer when depleted of anti-TNF- α antibody. Our future studies will target to

generate monodisperse porosity at different pore sizes. We expect that this will influence the diffusion dynamics of biologic agents from the DDS.

Conclusion

In conclusion, anti-TNF- α DDS made of PDMS/PVA polymers can be prepared and sterilized using gamma irradiation, providing an initial burst of biologically active antibody followed by zero-order release of low amounts of antibody for up to 1 month in vitro. The demonstrated long-term biological stability as well as in vivo tolerability of anti-TNF- α carrier polymer may facilitate future investigations targeting TNF- α as a modulator of various ocular surface diseases and may open the possibility of topical delivery of multiple biologic agents simultaneously.

Acknowledgments

Supported by grants from the Boston Keratoprosthesis Research Fund, Massachusetts Eye and Ear, and the Eleanor and Miles Shore Fund.

Disclosure: **M.-C. Robert**, None; **M. Frenette**, None; **C. Zhou**, None; **Y. Yan**, None; **J. Chodosh**, None; **F.A. Jakobiec**, None; **A.M. Stager**, None; **D. Vavvas**, None; **C.H. Dohlman**, None; **E.I. Paschalis**, None

References

- Martin D, Maguire M, Fine SL, et al; for the Comparison of Age-related Macular Degeneration Treatments Trials (CATT) Research Group. Ranibizumab and bevacizumab for treatment of neovascular age-related macular degeneration: two-year results. *Ophthalmology*. 2012;119:1388–1398.
- Chakravarthy U, Harding S, Rogers C, et al. Alternative treatments to inhibit VEGF in age-related choroidal neovascularisation: 2-year findings of the IVAN randomised controlled trial. *Lancet*. 2014;12:1258–1267.
- Das A, McGuire P, Rangasamy S. Diabetic macular edema: pathophysiology and novel therapeutic targets. *Ophthalmology*. 2015;122:1375–1394.
- Wells J, Glassman A, Ayala A, et al; for the Diabetic Retinopathy Clinical Research Network. Aflibercept, bevacizumab, or ranibizumab for diabetic macular edema. *N Engl J Med*. 2015; 372:1193–1203.
- Dastjerdi M, Al-Arfaj K, Nallasamy N, et al. Topical bevacizumab in the treatment of corneal neovascularization: results of a prospective, open-label, noncomparative study. *Arch Ophthalmol*. 2009;127:381–389.
- Hu Q, Qiao Y, Nie X, et al. Bevacizumab in the treatment of pterygium: a meta-analysis. *Cornea*. 2014;33:154–160.
- Vassileva P, Hergeldzhieva T. Avastin use in high risk corneal transplantation. *Graefes Arch Clin Exp Ophthalmol*. 2009;247:1701–1706.
- Leibovich S, Polverini P, Shepard H, et al. Macrophage-induced angiogenesis is mediated by tumour necrosis factor-alpha. *Nature*. 1987; 329:630–632.
- Li D-Q, Lokeshwar BL, Solomon A, et al. Regulation of MMP-9 production by human corneal epithelial cells. *Exp Eye Res*. 2001;73: 449–459.
- Ferrari G, Bignami F, Rama P. Tumor necrosis factor- α inhibitors as a treatment of corneal hemangiogenesis and lymphangiogenesis. *Eye Contact Lens*. 2015;41:72–76.
- Pham M, Chow C, Badawi D, et al. Use of infliximab in the treatment of peripheral ulcerative keratitis in Crohn disease. *Am J Ophthalmol*. 2011;152:183–188.e2.
- Thomas J, Pflugfelder S. Therapy of progressive rheumatoid arthritis-associated corneal ulceration with infliximab. *Cornea*. 2005;24:742–744.
- Odorcic S, Keystone EC, Ma JJK. Infliximab for the treatment of refractory progressive sterile peripheral ulcerative keratitis associated with late corneal perforation: 3-year follow-up. *Cornea*. 2009;28:89–92.
- Antao SF, Ayoub T, Tahir H, et al. Stabilization of bilateral progressive rheumatoid corneal melt with infliximab. *Case Rep Ophthalmol Med*. 2012; 2012:1–3.
- Dohlman J, Foster C, Dohlman C. Boston Keratoprosthesis in Stevens-Johnson Syndrome: a case of using infliximab to prevent tissue necrosis. *Digit J Ophthalmol*. 2009;15:1–6.
- Dohlman C, Dudenhofer E, Khan B, et al. Corneal blindness from end-stage Sjögren's syndrome and graft-versus-host disease. In: Sullivan D, Stern M, Tsubota K, et al., eds. *Lacrimal Gland, Tear Film, and Dry Eye Syndromes 3*. New York, NY: Kluwer/Plenum Publishers; 2002: 1335–1338.

17. Robert M, Crnej A, Shen L, et al. Infliximab after Boston Keratoprosthesis in Stevens-Johnson syndrome. An update. *Ocul Immunol Inflamm*. 2016; in press.
18. Cade F, Paschalis E, Regatieri C, et al. Alkali burn to the eye: protection using TNF- α inhibition. *Cornea*. 2014;33:382–389.
19. Ferrari G, Bignami F, Giacomini C, et al. Safety and efficacy of topical infliximab in a mouse model of ocular surface scarring. *Invest Ophthalmol Vis Sci*. 2013;54:1680–1688.
20. Li Z, Choi W, Oh H-J, et al. Effectiveness of topical infliximab in a mouse model of experimental dry eye. *Cornea*. 2012;31(suppl 1):S25–S31.
21. Kim JW, Chung SK. The effect of topical infliximab on corneal neovascularization in rabbits. *Cornea*. 2013;32:185–190.
22. Turgut B, Eren K, Akin M, et al. Topical infliximab for the suppression of wound healing following experimental glaucoma filtration surgery. *Drug Des Devel Ther*. 2014;2:421–429.
23. Seet R, Rabinstein A, Lindell P, et al. Cerebrovascular events after bevacizumab treatment: an early and severe complication. *Neurocrit Care*. 2011;15:421–427.
24. Jain A, Singh J. Harms of tumor necrosis factor inhibitors in rheumatic diseases: a focused systematic review of the literature. *Immunotherapy*. 2013;5:265–299.
25. Jansen Biotech I. Remicade prescribing information. Secondary Remicade prescribing information. Available at: <http://www.remicade.com/shared/product/remicade/prescribing-information.pdf>. Access March 2, 2016.
26. Poku E, Rathbone J, Wong R, et al. The safety of intravitreal bevacizumab monotherapy in adult ophthalmic conditions: a systematic review. *BMJ Open*. 2014;4:e005244.
27. Genentech. Avastin (bevacizumab) prescribing information. Secondary Avastin (bevacizumab) prescribing information Available at: <http://www.avastin-hcp.com>. Access March 2, 2016.
28. Patel A, Cholkar K, Agrahari V, et al. Ocular drug delivery systems: an overview. *World J Pharmacol* 2013;2:47–64.
29. Walsh G. *Proteins: Biochemistry and Biotechnology*. 2nd Edition. Limerick, Ireland: Wiley-Blackwell; 2014.
30. Pisal D, Kosloski M, Balu-Iyer S. Delivery of therapeutic proteins. *J Pharm Sci* 2010;99:2557–2575.
31. Paschalis E, Elliott D, Vavvas D. Removal of silicone oil from intraocular lens using novel surgical materials. *Transl Vis Sci Technol*. 2014; 3(5):4.
32. Ikeda R, Vermeulen LC, Lau E, et al. Stability of infliximab in polyvinyl chloride bags. *Am J Health Syst Pharm*. 2012;69:1509–1512.
33. Robert M, Spurr-Michaud S, Frenette M, et al. Stability and in vitro toxicity of an infliximab eye drop formulation. *Int J Pharm Compd*. 2014;18: 418–426.
34. Dastjerdi M, Sadrai Z, Saban D, et al. Corneal penetration of topical and subconjunctival bevacizumab. *Invest Ophthalmol Vis Sci*. 2011;52: 8718–8723.
35. Ako-Adounvo A, Nagarwal R, Oliveira L, et al. Recent patents on ophthalmic nanoformulations and therapeutic implications. *Recent Pat Drug Deliv Formul*. 2014;8:193–201.
36. Bengani L, Hsu K, Gause S, et al. Contact lenses as a platform for ocular drug delivery. *Expert Opin Drug Delivery*. 2013;10:1483–1496.
37. Ciolino J, Dohlman C, Kohane D. Contact lenses for drug delivery. *Semin Ophthalmol*. 2009;24: 156–160.
38. Guzman-Aranguiz A, Colligris B, Pintor J. Contact lenses: promising devices for ocular drug delivery. *J Ocul Pharmacol Ther*. 2013;29:189–199.
39. Aburahma M, Mahmoud A. Biodegradable ocular inserts for sustained delivery of brimonidine tartarate: preparation and in vitro/in vivo evaluation. *AAPS Pharm Sci Tech*. 2011;12: 1335–1347.
40. Pollack I, Quigley H, Harbin T. The Ocusert pilocarpine system: advantages and disadvantages. *South Med J*. 1976;69:1296–1298.
41. Peppas N, Simmons R. Mechanistic analysis of protein delivery from porous poly(vinyl alcohol) systems. *J Drug Del Sci Tech*. 2004;14:285–289.
42. Vashist A, Ahmad S. Hydrogels: smart materials for drug delivery. *Oriental Journal of Chemistry*. 2013;29:861–870.
43. Mashak A, Rahimi A. Silicone polymers in controlled drug delivery systems: a review. *Iranian Polymer Journal*. 2009;18:279–295.
44. Walsh G. *Biopharmaceuticals: Biochemistry and Biotechnology*. Limerick, Ireland: Wiley; 2013.
45. Alvarez S, Blanco A, Fresno M, et al. TNF- α contributes to caspase-3 independent apoptosis in neuroblastoma cells: role of NFAT. *PLoS One*. 2011;6:e16100.
46. Kastellorizios M, Tipnis N, Burgess D. Foreign body reaction to subcutaneous implants. *Adv Exp Med Biol*. 2015;865:93–108.